ISBN: 978-3-95450-222-6 ISSN: 2673-5350 doi:10.18429/JACoW-IBIC2020-WEPP20

MEASUREMENTS OF ULTRAVIOLET FEL SEED LASER PULSE WIDTH BROADING IN THIN β-BBO CRYSTALS*

Chunlei Li[1], Xingtao Wang, Wenyan Zhang, Lie Feng, Bo Liu†
Shanghai Advanced Research Institute, Chinese Academy of Science, Shanghai, China
[1] also at Shanghai Institute of Applied Physics, Chinese Academy of Science, Shanghai, China

Abstract

Short pulse, high power seed lasers have been implemented to improve the longitudinal coherence and shot-to-shot reproducibility of Free Electron Lasers (FEL). The laser pulse duration is typically 100 - 200 fs with wavelengths in the 260 nm range produced from third harmonic generation of a Ti:sapphire laser. The pulse duration must be measured accurately for seeded FEL operation. The Ultraviolet (UV) pulse width measurement can be carried out with intensity cross-correlation based on the difference frequency generation (DFG) in ultrathin β-Barium Borate (BBO) crystals. The DFG output pulse broadened due to group velocity mismatch between the 266.7 nm and 800 nm components. The broadening effect depends on the BBO crystal thickness so we explored 0.015 mm, 0.055 mm and 0.1 mm thick samples. To the best of our knowledge, this is the first time that β-BBO crystal with thickness of only 0.015 mm has been used to measure the UV seed laser pulse width. Experiment results show the measured pulse width broadens with increased BBO thickness in agreement with a theoretical model.

INTRODUCTION

Particle accelerator and laser technologies are effectively combined in FEL facilities, with the latter being a key factor determining the ultimate performance [1]. Laser technology is used at many strategic points: (1) cathode drive laser (257-267 nm, 5-30 ps) to create the electron bunch, (2) laser heater (400-1030 nm, 15-20 ps) to increase beam energy spread [2], and (3) seed laser (210-280 nm, 90-300 fs) to improve longitudinal coherence and reproducibility of the FEL output [3].

Two-beam cross correlation can be used to characterize the temporal structure of photocathode drive laser pulse [4-7] and the resulting electron bunch length [8]. The drive laser pulse width is in a range of 5-50 ps, so pulse broadening caused by the group velocity mismatch (GVM) in ultrathin (<0.1 mm) BBO crystal is negligible. However, pulse broadening has to be understood when measuring the seed laser pulse in the range of 100-300 fs.

In this paper, pulse broadening was experimentally investigated using β-BBO crystals with three different thicknesses to experimentally determine the effect of GVM on the measurement. Ultrathin crystals with thickness of only 0.015 mm were found to have the least broadening effect.

*This study was sponsored by Shanghai Sailing Program (18YF1428700).
†Corresponding author: liubo@zjlab.org.cn

SEED LASER SYSTEM

Figure 1 shows a schematic for Shanghai soft X-ray free electron laser (SXFEL) seed laser system. The laser consists of 4 main stages: (1) Oscillator, (2) Amplifier, (3) third harmonic generation (THG), and (4) beam transport line. The oscillator (Vitara-T, Coherent Inc.) is pumped by a 4.88 W green CW Verdi laser (Coherent Inc.) to deliver a 0.7 W stream of 79.33 MHz pulses at 800 nm with horizontal polarization to a synchronized regenerative Ti:Sapphire amplifier (Elite Duo, Coherent Inc.). The pre-amplified oscillator pulses have 7nJ energy and are stretched to 200 ps using a grating pair, then amplified by the regen and recompressed (CPA system). The output has 3 mJ in 100 fs (FWHM). The infrared (IR) pulses are then tripled to 266.7 nm with 300 μJ and a bandwidth of 0.8 nm. The UV light is then transported to the main FEL undulator through vacuum beam transport lines.

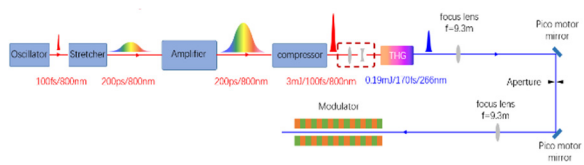

Figure 1: Schematic of SXFEL seed laser system.

The structure of THG optics is shown in Fig. 2. Here the compressed IR pulse is frequency-doubled to 400 nm in a β-BBO crystal (type I, o + o = e, 0.5 mm, θ =29.2°), and subsequently undergoes sum-frequency generation when re-mixed with 800 nm in a second β-BBO crystal (type I, 0.5 mm, θ=44.4°). The conversion efficiency from 800 nm to 266 nm was about 10%. The 266.7 nm UV pulse width was measured by co-linear cross correlation as presented in the following section.

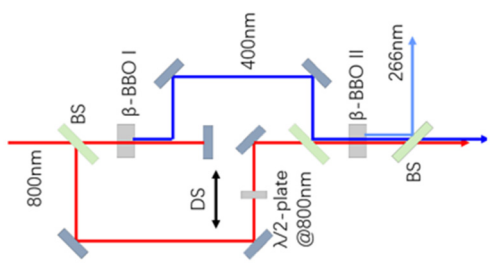

Figure 2: Structure of third harmonic generation (THG) device. BS-beam splitter; DS-delay stage.

ISBN: 978-3-95450-222-6 ISSN: 2673-5350 doi:10.18429/JACoW-IBIC2020-WEPP20

THEORETIC FRAMEWORK FOR THE CROSS CORRELATION MEASUREMENT

For the collinear cross correlation measurement, three light waves travel through the crystal in the same direction. Due to the fact that the β-BBO medium is a negative-uniaxial crystal ($n_e < n_o$), the three waves travel at different phase velocities corresponding to different refractive indices n_{IR}, n_{DFG}, n_{UV}. The frequency and phase matching conditions are expressed in Eqs. (1) and (2) which must be satisfied simultaneously.

$$\omega_{IR} + \omega_{DFG} = \omega_{UV} \tag{1}$$

$$n_{IR}\omega_{IR} + n_{DFG}\omega_{DFG} = n_{UV}\omega_{UV} \tag{2}$$

where n_{IR}, n_{UV}, and n_{DFG} are the refraction indices for 800nm, 266.7nm and 400nm light. ω_{IR}, ω_{UV} and ω_{DFG} are frequencies of the above three wavelengths.

Within the anisotropic β -BBO crystal, the three refractive indexes n_{IR} , n_{DFG} , n_{UV} are dependent on frequency, field polarization and propagation direction relative to the principal axes. This offers a set of free variables that can be manipulated to satisfy the matching conditions. Precise control of the refractive indexes at all three frequencies can be achieved by appropriate selection of field polarization and beam orientation in the BBO crystal.

β-BBO has a uniaxial crystal structure characterized by its optic axis and frequency dependent ordinary and extraordinary refractive indexes $n_o(\omega)$ and $n_e(\omega)$. For an o-wave $n(\omega) = n_o(\omega)$; for an e wave $n(\omega) = n_e(\theta, \omega)$ also depends on the angle θ between the direction of the wave and the optic axis of the crystal, which is shown in Fig.3. and expressed in Eq.(3) [9].

$$\frac{1}{{n_e}^2(\theta,\omega)} = \frac{\cos^2\theta}{{n_o}^2(\omega)} + \frac{\sin^2\theta}{{n_e}^2(\omega)} \tag{3}$$

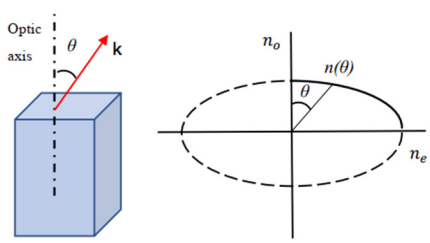

Figure 3: Refractive index $n(\theta)$ of the extraordinary wave. θ is the angle between the optic axis and the direction of propagation. Vector k shows beam propagation direction.

For the cross correlation measurements discussed here with different BBO crystal thicknesses, the output DFG signal intensity is correlated with the temporal delay between the IR and UV pulses. The cross-correlation overlap integral for intensity output can be expressed as Eq. (4) [10]:

$$I(\tau)_{cc} = \alpha \int_{-\infty}^{\infty} I_{uv}(t) I_{IR}(t-\tau) dt \tag{4}$$

where $I_{uv}(t)$ and $I_{IR}(t-\tau)$ are the temporal intensities for the two input beams, τ is the time delay between them, α is an overall conversion efficiency factor and $I(\tau)_{cc}$ is the output signal intensity of the 400 nm DFG output pulse.

By assuming ideal light pulses with Gaussian distribution along with negligible frequency chirp and negligible group velocity mismatch, the full width at half maximum (FWHM) τ_{cc} of the output envelope is:

$$\tau_{cc} = \sqrt{\tau_{IR}^2 + \tau_{UV}^2} \tag{5}$$

Since τ_{IR} can be directly measured by intensity auto correlation, τ_{UV} can be derived from measurement of τ_{cc}.

More generally, if one of the input beam profiles is known and we measure $I(\tau)_{cc}$, then a more accurate result for the unknown beam profile can be derived by numerical deconvolution according to Eq.(6). Specifically, we include the effects of both the group velocity mismatch (GVM) between two input pulses and the thickness of BBO crystal [11, 12] in the integration. The GVM roughly broadens the output pulse by a linear factor $\delta t = L * GVM$, where L is the thickness of BBO crystal for collinear propagation [13]. To estimate the input pulse width in this case, the broadening value δt has to be deduced from the pulse width of the 400 nm output signal. Then the UV input pulse width can be derived by deconvolution according to Eq. (5).

$$I_{cc}(\tau) \approx \int_{-\infty}^{\infty} \left\{ \exp\left[-2ln2 \left(\frac{t}{\tau_{UV}} \right)^2 \right] \right\}^2 \times \left\{ exp\left[-2ln2 \left(\frac{t-\tau}{\tau_{IR}} \right)^2 \right] \otimes sqr\left[\frac{t}{\Delta\left(v_g^{-1}\right)_{cc} l_c} + \frac{1}{2} \right] \right\}^2 dt \tag{6}$$

In Eq. (6)

$$sqr(x) = \begin{cases} 1, & |x| \le 1/2 \\ 0, & otherwise \end{cases},$$

τ_{UV} is the FWHM pulse width of UV beam, and τ_{IR} is the FWHM pulse width of IR beam. $\Delta\left(v_g^{-1}\right)_{cc}$ is the GVM between the UV and IR beams, l_c is the thickness of β-BBO crystal and ⊗ denotes convolution. The expression for group velocity and group velocity mismatch are given by in Eq. (7) and (8), respectively [14]:

ISBN: 978-3-95450-222-6 ISSN: 2673-5350 doi:10.18429/JACoW-IBIC2020-WEPP20

$$v_g = \frac{c}{n}\left(1 + \frac{\lambda}{n}\frac{dn}{d\lambda}\right) \quad (7)$$

$$\Delta\left(v_g^{-1}\right)_{cc} = \mathrm{GVM} = \frac{1}{V_g^{IR\_o}} - \frac{1}{V_g^{UV\_e}} \quad (8)$$

Here c is the speed of light, λ is wavelength in μm, $V_g^{IR\_o}$ is the IR o-ray group velocity, $V_g^{UV\_e}$ is the e-ray UV group velocity with a crystal cutting angle θ =44.4 °. n is refractive index of the BBO crystal. The refractive indices for the *o*-ray and *e*-ray in BBO can be calculated according to Eq. (9) and Eq. (10) [15-17]. These parameters were also cross-checked using SNLO software [18].

$\frac{dn_o(\lambda)}{d\lambda}$ and $\frac{dn_e(\lambda)}{d\lambda}$ are expressed in Eq. (11) and Eq. (12).

The refraction indices for a 266.7 nm e-ray propagating through the BBO crystal with a cutting angle $\theta = 44.4°$ were calculated using Eqs. (3), (9) and (10).

$$n_o(\lambda) = \sqrt{2.7405 + \frac{0.0184}{\lambda^2 - 0.0179} - 0.0155\lambda^2} \quad (9)$$

$$n_e(\lambda) = \sqrt{2.3730 + \frac{0.0128}{\lambda^2 - 0.0156} - 0.0044\lambda^2} \quad (10)$$

$$\frac{dn_o(\lambda)}{d\lambda} = \frac{1}{2} * \frac{-\frac{0.0184}{(\lambda^2 - 0.0179)^2} * 2\lambda - 0.0155 * 2\lambda}{\sqrt{2.7405 + \frac{0.0184}{\lambda^2 - 0.0179} - 0.0155\lambda^2}} \quad (11)$$

$$\frac{dn_e(\lambda)}{d\lambda} = \frac{1}{2} * \frac{-\frac{0.0128}{(\lambda^2 - 0.0156)^2} * 2\lambda - 0.0044 * 2\lambda}{\sqrt{2.3730 + \frac{0.0128}{\lambda^2 - 0.0156} - 0.0044\lambda^2}} \quad (12)$$

CROSS-CORRELATION MEASUREMENT

In order to explore pulse broadening for different β-BBO crystal thicknesses, a DFG cross correlator was constructed as shown in Fig. 4.

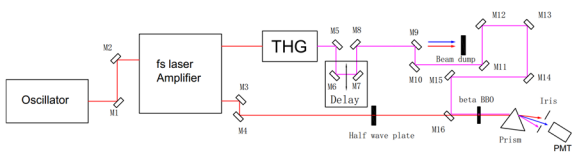

Figure 4: Schematic of the collinear cross-correlation diagnostic system. A prism was used to spatially separate the frequency components at the output stage.

The 800 nm IR pulses from the Vitara oscillator have a bandwidth of 50 nm and pulse energy of about 1 nJ. The UV beam is produced by the THG tripler shown in Fig. 2. The THG beam is filtered by dichroic mirror M9 and the 800 nm and 400 nm components are directed to beam blocks. The UV beam is directed to the β-BBO crystal (CASTECH, type I phase matched at θ = 44.4°, ϕ= 0°) by M10-M16. M16 is dichroic mirror where the UV and IR beams spatially overlap. M6 and M7 were installed on high precision delay stages (M-ILS200CCL, Newport) to adjust the UV beam arrival time for temporal overlap with the IR beam. In order to meet the phase match conditions in the β-BBO crystal, a half wave plate was inserted in the beam path to rotate the IR beam polarization into the vertical plane. Three β-BBO crystals with different thicknesses of 0.1 mm, 0.055 mm and 0.015 mm were tested to study VGM pulse broadening effects.

To separate the three output beams, a fused silica prism was inserted as shown in Fig.4. An iris with diameter ~1mm and a bandpass filter (Semrock, FF01-389/3-25) were installed after the prism to reduce background noise. By adjusting UV pulse arrival time with the adjustable delay stage, the 400 nm pulse intensity cross correlation envelope was measured at a photomultipler tube (PMT) (Hamamatsu, H10711-210). The PMT position was adjusted with a kinematic V-clamp (Thorlab, KM200V/M) and the data was acquired on an integrating oscilloscope (Tektronix, DPO4054). The scan motion of delay stage and DFG signal acquisition were then correlated in a LabVIEW gui interface.

RESULTS AND DISCUSSION

The intensity cross correlation curves for the 400 nm DFG signal using three different β -BBO crystal thicknesses are plotted in Figs. 5 (a-c). The horizontal axis is the temporal delay between two input beams and vertical axis is the normalized signal intensity. The experiment data are plotted in blue dots with error bars. In order to derive the FWHM value of the data curve, nonlinear least-squares fitting was performed with the Levenberg-Marquardt algorithm. The simulated curves calculated by Eq. (6) are also shown in Figs. 5 (a-c) (red curve) and the corresponding FWHM values are plotted in Fig. 6.

Our cross correlation measurements performed with three β-BBO crystals of thickness 0.015 mm, 0.055 mm and 0.1mm. The FWHM pulse widths of the corresponding cross correlation signals were 248 fs, 272 fs and 307 fs, respectively. As the BBO thickness increases, the FWHM of measured cross correlation signal broadens due to the GVM effect. The measured data plotted in Fig.5 (a-c) (blue line) was fitted using Eq. (6) with τ_{IR}=57 fs, τ_{UV}=248 fs yielding $\Delta\left(v_g^{-1}\right)_{cc}$ = 671.5 fs/mm. Furthermore, we believe that we can reliably extract the broadened UV pulse width by deconvolution from the cross correlation data.

ISBN: 978-3-95450-222-6 ISSN: 2673-5350 doi:10.18429/JACoW-IBIC2020-WEPP20

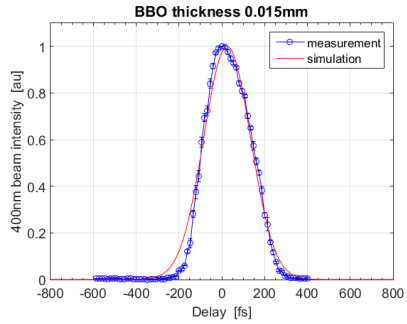

(a)

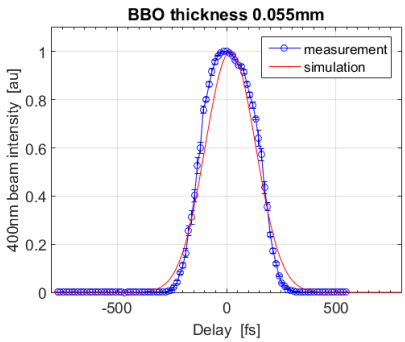

(b)

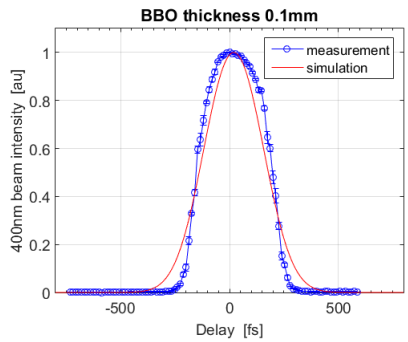

Figure 5: Cross correlation data with error bars (blue line) and numerical fits (red line) using 0.015 mm, 0.055 mm, and 0.1 mm β-BBO crystal for DFG. All curves are fitted by Eq. (6) with τ_{IR}=57 fs, τ_{UV}=248 fs, and $\Delta\left(v_g^{-1}\right)_{cc}$= 671.5 fs/mm.

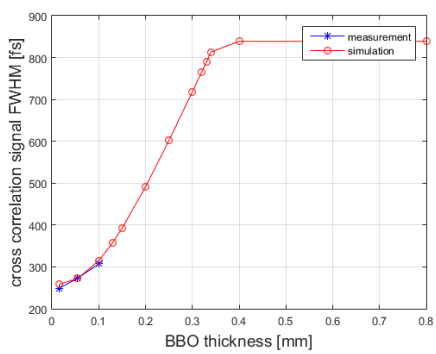

Figure 6: FWHM of cross correlation signal from data in Fig 5. For these data Eq. (6) with τ_{IR}=57 fs, τ_{UV}=248 fs, and $\Delta\left(v_g^{-1}\right)_{cc}$= 671.5 fs/mm.

CONCLUSION

In conclusion, pulse broadening of the 400 nm DFG cross-correlation signal was experimentally investigated in three different β-BBO crystal thicknesses. The data includes the most thin 0.015 mm BBO crystal thickness measurements for the first time to our knowledge. The results show that the 400nm DFG pulse width increases as the BBO thickness increases as predicted. For the case with a 0.055 mm crystal the measured ~272 fs FWHM pulse length is in very good agreement with theory and the two other measurements are within a about 4 percent.

The results agree well with the theoretical model integrating over β-BBO thickness with group velocity modulation as a function of wavelength taken into consideration. In practice, dispersion, spatial chirp and other nonlinear mechanisms also play important roles in pulse broadening. Therefore, further study are underway to explore their influence.

ACKNOWLEDGMENTS

The authors would like to thank Jeff Corbett for his precious comments and the proofreading of the manuscript, M.B. Danailov for constructive discussions, and Guorong Wu and his group in Dalian coherent light source for fruitful discussions converning the PMT device.

This work was sponsored by Shanghai Sailing Program (18YF1428700).

REFERENCES

[1] M.B. Danailov, A. Demidovich, R. Ivanov, I. Nikolov, and P. Sigalotti, "Laser systems for next generation light sources", in *Proc. 23rd Particle Accelerator Conf. (PAC'09)*, Vancouver, BC, Canada, May. 2009, paper MO4GRI03, pp. 122-126.

[2] S. Gilevivch *et al.*, "LCLS-II gun and laser heater systems", LCLS-II-2.2-PR-0085-R1, 2017.

[3] M. B. Danailov *et al.*, "Design and first experience with the fermi seed laser", in *Proc. 33rd Int. Conf. on Free Electron Laser (FEL'11)*, Shanghai, China, Aug. 2011, paper TUOC4, pp. 183-186.

[4] J. Good *et al.*, "Preliminary on–table and photo-electron results from the PIZT quasi-ellipsoidal photocathode laser system", in *Proc. 38th Int. Conf. on Free Electron Laser (FEL'17)*, Santa Fe, NM, USA, Aug. 2017, pp. 418-420. doi:10.18429/JACoW-FEL2017-WEPO06

[5] Dong Wang, Lixin Yan, and Wenhui Huang, "UV pulse shaping with α-BBO crystals for the photocathode RF gun", in *Proc. 7th Int. Particle Accelerator Conf. (IPAC'16)*, Busan, Korea, May 2016, pp. 4079-4081. doi:10.18429/JACoW-IPAC2016-THPOW059

[6] Lixin Yan *et al.*, "Measurements of laser temporal profile and polarization dependent quantum efficiency", in *Proc. 22nd Particle Accelerator Conf. (PAC'07)*, Albuquerque, NM, USA, Jun. 2007, paper TUPMN056, pp. 1052-1054.

[7] T. Rublack *et al.*, "Development of a quasi 3D ellipsoidal photocathode laser system for PIZT", in *Proc. 5th Int. Particle Accelerator Conf. (IPAC'14)*, Dresden, Germany, Jul. 2014, pp. 2069-2071. doi:10.18429/JACoW-IPAC2014-WEPRO055

ISBN: 978-3-95450-222-6 ISSN: 2673-5350 doi:10.18429/JACoW-IBIC2020-WEPP20

[8] T. Miller *et al.*, "Bunch length measurements with laser/SR cross correlation", in *Proc. 1st Int. Particle Accelerator Conf. (PAC'10)*, Kyoto, Japan, May 2010, paper WEOCMH03, pp. 2408-2410.

[9] Bahaa E.A. Saleh and Malvin Carl Teich, "Polarization Optics" in *Fundamentals of Photonics*, Bahaa E.A. Saleh, Ed, Second Edition, Hoboken, New Jersey, USA: Wiley Wiley, 2007, pp. 220-221.

[10] Andrew M. Weiner, "Ultrafast pulse measurement methods" in Ultrafast Optics, Glenn Boreman Ed, Hoboken, New Jersey, USA: Wiley, 2009, pp. 100-110.

[11] Jing Yang *et al.*, "Pulse broadening of deep ultraviolet femtosecond laser from second harmonic generation in $KB_2BO_3F_2$ crystal", *Optics Communications*, vol. 288, pp: 114-117, 2013.

[12] D. C. Edelstein *et al.*, "Femtosecond ultraviolet pulse generation in β-BaB_2O_4", *Appl. Phys. Lett.,* vol. 52, no.26, pp. 2211-2213, 1988.

[13] D. Gutierres Cornoel, "Analysis of auto and cross correlator", Lee Teng Intership Paper, Department of Physics, Illinois Institute of Technology, USA, Aug. 2017.

[14] Eugene Hecht, "The superposition of waves" in Optics, Fifth Edition, Eugene Hecht Ed, Person Education, 2017, pp. 304-306.

[15] John G. Power, and Chunguang Jing, "Temporal laser pulse shaping for RF photocathode guns: the cheap and easy way using UV birefringent crystals", in *Proc. 13th Workshop on Advanced Accelerator Concepts (ACC'08)*, Santa Cruz, CA, USA, Jan. 2009, pp. 689-694.

[16] D. N. Nikogosyan, "Beta barium borate (BBO)", *Appl. Phys. A*, vol. 52, pp. 359–368, 1991.

[17] X. T. Wang *et al.*, "Drive laser temporal shaping techniques for Shanghai soft X ray free electron laser", in *Proc. 39th Conf. on Free Electron Laser (FEL'19)*, Hamburg, Germany, Aug. 2019, pp. 466-468. doi:10.18429/JACoW-FEL2019-WEP058

[18] A. V. Smith, "How to select nonlinear crystals and model their performance using SNLO software", in *Proc. SPIE vol 3928, Nonlinear Materials, Devices, and Applications*, Mar. 2000, San Jose, CA, USA, pp. 1-8.